Journal of Nuclear Materials 541 (2020) 152410

Contents lists available at ScienceDirect

Journal of Nuclear Materials

journal homepage: www.elsevier.com/locate/jnucmat

Modelling and assessment of thermal conductivity and melting behaviour of MOX fuel for fast reactor applications

A. Magni[a], T. Barani[a], A. Del Nevo[b], D. Pizzocri[a], D. Staicu[c], P. Van Uffelen[c,*], L. Luzzi[a]

[a] Politecnico di Milano, Department of Energy, Nuclear Engineering Division, via La Masa 34, 20156, Milano, Italy
[b] ENEA, FSN-ING-SIS, CR Brasimone, 40032, Camugnano (BO), Italy
[c] European Commission, Joint Research Centre, Directorate for Nuclear Safety and Security, P.O. Box 2340, 76125, Karlsruhe, Germany

ARTICLE INFO

Article history:
Received 20 April 2020
Revised 22 June 2020
Accepted 18 July 2020
Available online 25 July 2020

Keywords:
Nuclear fuel
MOX
Thermal conductivity
Melting
Fast reactor

ABSTRACT

Thermal conductivity and melting temperature of nuclear fuel are essential for analysing its performance under irradiation, since they determine the fuel temperature profile and the melting safety margin, respectively. A starting literature review of data and correlations revealed that most models implemented in state-of-the-art fuel performance codes (FPCs) describe the evolution of thermal conductivity and melting temperature of Light Water Reactor (LWR) MOX (uranium-plutonium mixed oxide) fuels, in limited ranges of operation and without considering the complete set of fundamental dependencies (i.e., fuel temperature, burn-up, plutonium content, stoichiometry, and porosity). Since innovative Generation IV nuclear reactor concepts (e.g., ALFRED, ASTRID, MYRRHA) employ MOX fuel to be irradiated in Fast Reactor (FR) conditions, codes need to be extended and validated for application to design and safety analyses on fast reactor MOX fuel. The aim of this work is to overcome the current modelling and code limitations, providing fuel performance codes with suitable correlations to describe the evolution under irradiation of fast reactor MOX fuel thermal conductivity and melting temperature. The new correlations have been obtained by a statistically assessed fit of the most recent and reliable experimental data. The resulting laws are grounded on a physical basis and account for a wider set of effects on MOX thermal properties (fuel temperature, burn-up, deviation from stoichiometry, plutonium content, porosity), providing clear ranges of applicability for each parameter considered. As a first test series, the new correlations have been implemented in the TRANSURANUS fuel performance code, compared to state-of-the-art correlations, and assessed against integral data from the HEDL P-19 fast reactor irradiation experiment. The integral validation provides promising results, pointing out a satisfactory agreement with the experimental data, meaning that the new models can be efficiently applied in engineering fuel performance codes.

Acronyms

ALFRED	Advanced Lead-cooled Fast Reactor European Demonstrator
ASTRID	Advanced Sodium Technological Reactor for Industrial Demonstration
EBR	Experimental Breeder Reactor
EPMA	Electron Probe MicroAnalysis
ESFR-SMART	European Sodium Fast Reactor - Safety Measures Assessment and Research Tools
ESNII	European Sustainable Nuclear Industrial Initiative
FBR	Fast Breeder Reactor
FPC	Fuel Performance Code
FR	Fast Reactor
HEDL	Hanford Engineering Development Laboratory
HM	Heavy Metal
HRP	Halden Reactor Project
IFPE	International Fuel Performance Experiments
INSPYRE	Investigations Supporting MOX Fuel Licensing for ESNII Prototype Reactors
LHR	Linear Heat Rate
LWR	Light Water Reactor
MIMAS	MIcronized - MASter blend
MOX	Mixed-OXide
MYRRHA	Multi-purpose hYbrid Research Reactor for High-tech Applications
O/M	Oxygen/Metal ratio
OD	Outer Diameter
OECD/NEA	Organisation for Economic Co-operation and Development / Nuclear Energy Agency

* Corresponding author.
E-mail address: Paul.VAN-UFFELEN@ec.europa.eu (P. Van Uffelen).

https://doi.org/10.1016/j.jnucmat.2020.152410

PIE	Post-Irradiation Examination
rmse	root mean square error
SBR	Short Binderless Route
TD	Theoretical Density
XANES	X-ray Absorption Near Edge Structure
XRD	X-Ray Diffraction

1. Introduction

The development of Generation IV reactor concepts, employing uranium-plutonium mixed oxide (MOX[1]) fuel irradiated under fast neutron flux, calls for dedicated and advanced fuel modelling with respect to the state of the art (target of the INSPYRE H2020 Project [1]). In particular, accurate models of fuel thermal conductivity and melting (solidus) temperature evolution under irradiation are of great importance, to correctly evaluate the fuel temperature profile (impacting on both thermal and mechanical behaviour) and the margin to melting – one of the most important safety design criteria [2–4]. The current modelling of thermal properties of fast reactor MOX in fuel performance codes (FPCs, e.g., GERMINAL [5], TRANSURANUS [6], BISON [7], FEMAXI [8]) is limited, for various reasons. First, available experimental data regard fresh MOX or LWR irradiation conditions, while only very few data correspond to irradiated fast reactor MOX. Second, the main existing correlations, validated and employed by FPCs, consider the temperature, porosity and burn-up effects on MOX thermal conductivity, without accounting, for instance, for the effect of the initial plutonium content [6,9,10]. The current melting temperature correlations do not incorporate in an assessed way the effects of plutonium content, deviation from fuel stoichiometry and burn-up [6]. The minor actinide content (americium and neptunium especially) and its impact on MOX thermal properties is also of great relevance, in view of MOX application in Generation IV fast breeder reactors [11–13]. The analysis of minor actinide-bearing MOX is beyond the scope of the present work and will be considered in a following step.

Up to now, MOX fuel has been the object of several researches (albeit limited if compared to those concerning UO_2 nuclear fuel), often showcasing conflicting conclusions amongst the different authors. The effect of the plutonium content on the thermal conductivity of fresh U-Pu mixed oxides was already studied in early experimental works (e.g., Gibby [14] and Schmidt (1969), Serizawa et al. (1970), Goldsmith et al. (1972), reviewed by Bonnerot [15]). While Gibby shows a decrease of the thermal conductivity with increasing plutonium content (less pronounced as temperature increases towards 1500 K), down to a minimum occurring at around 70 wt.% Pu, Goldsmith and co-workers support a linear decrease of the thermal conductivity between 0 and 30 wt.% Pu (at low temperatures between 700 K and 1300 K). Instead, both Schmidt and Serizawa et al. claim that the plutonium content has no influence on MOX thermal diffusivity and conductivity (at temperatures above 1300 K and in the entire temperature range, respectively). Concerning the effect of stoichiometry deviation on the fuel thermal conductivity, it has been the specific focus of investigations by some early works on fresh MOX reported by Bonnerot [15] (Van Craeynest et al. (1968), Weilbacher (1972), Laskiewicz et al. (1971)), again showing conflicting results. Weilbacher measurements highlight a constant effect of the deviation from fuel stoichiometry (i.e., from oxygen-to-metal ratio, O/M, equal to 2.00) on the thermal conductivity over the entire temperature range (from 800 to 3000 K), while Van Craeynest et al. and Laskiewicz et al. agree on a substantial effect on hypo-stoichiometric fuel at low temperatures, which becomes negligible at high temperatures (i.e., same thermal conductivity value at ~ 2000 K, independently on the O/M ratio).

The aforementioned experimental works have been exploited to build models of MOX fuel thermal conductivity for fast reactor applications, developed e.g., by Bonnerot [15] and Philipponneau [9], based on the comprehensive review of thermal properties of oxide fuels carried out by Martin [16]. They showed that in the wide temperature range between 800 and 3100 K the MOX thermal conductivity is always lower with respect to UO_2, with only slight effects of plutonium concentration (below 12 wt.%) in the entire temperature range, and of O/M ratio at high temperatures. Inoue [17] proposed a model that was integrally validated against data from pin irradiation experiments in the JOYO reactor. More recent works focused on the experimental characterization and modelling of thermal conductivity of both fresh and irradiated LWR MOX, featured by a low plutonium content up to 15 wt.%, e.g., [18–22]. Instead, recent and up-to-date measurements on fresh fast reactor MOX have been performed on fuel samples from PHENIX (~ 24 wt.% Pu, stoichiometric, at temperatures < 1650 K) and TRABANT (~ 40 and 45 wt.% Pu, O/M from 1.96 to 2.00, at temperatures < 1650 K), in the framework of the ESNII+ H2020 Project [23,24]. In the latter, the temperature effect has been the focus, and indeed two correlations were derived specifically for PHENIX and TRABANT MOX fuel, accounting only for the temperature effect. As for irradiated fast reactor MOX, the only accessible experimental measurements of thermal conductivity have been performed by Yamamoto et al. [25] and by the ESNII+ Project on NESTOR-3 fuel samples [26] (both fuels with ~ 20 wt.% Pu, but irradiated at moderate and high burn-up, i.e., up to 35 GWd/tHM and 84 and 130 GWd/tHM, respectively). The conclusions of both works shed only partial light on the behaviour of thermal conductivity as a function of fuel burn-up. Indeed, the degradation of FR MOX thermal conductivity as burn-up increases has not been definitely proven from experimental observations, since the measured effect of low and moderate burn-up is slight [25], while at very high burn-up the MOX thermal conductivity seems to be higher [26]. The lack of sufficient, concordant, and highly reliable experimental data can be indicated as the reason why existing thermal conductivity correlations do not represent all the effects experimentally observed (temperature, burn-up, plutonium content, deviation from stoichiometry, porosity).

As for the state-of-the-art about the melting temperature, early experimental works have been performed by Lyon and Baily on fresh stoichiometric MOX with a plutonium content up to 85 mol.% [27], by Aitken, Evans (1968) and Reavis (1972), and reported in [28]. The latter included both fresh and low burn-up MOX, with oxygen-to-metal ratio between 1.97 and 2.00 and a plutonium content up to 60 mol.%. The melting temperature measured in these early campaigns resulted in values sensibly lower than expected, and was therefore re-assessed. As a result, it has been proven that a tungsten melting capsule strongly contaminates the melted fuel specimen and heavily lowers the observed melting temperature [29,30]. Other melting experiments performed in tungsten capsules, employing the thermal arrest technique, have been performed on irradiated fast reactor MOX fuel [25,30–32], on fresh MOX [29,33], and on both fresh and irradiated MOX [34,35].

More recent experimental campaigns employed rhenium melting capsules (at least with an inner rhenium layer), to avoid the distortion of the measured melting temperature [33,35]. Nevertheless, the most up-to-date experimental technique uses laser heating of the sample (e.g., [36,37]), leading to accurate measurements performed on fresh MOX fuel with high Pu content [23,38–40] (up to 90 mol.%) and featuring also a small inclusion of americium (up to 3.5 mol.%) [40]. Experimental results on Am-MOX are also included in older works by Konno et al. [32,34] and Kato et al. [33] (americium content up to 0.9 and 3.3 mol.%, respectively).

[1] The term MOX is herein used referring both to the $(U,Pu)O_2$ homogeneous fuel envisaged for fast reactor applications and to the heterogeneous uranium and plutonium mixed oxide fuel employed in LWRs.

Table 1
List of selected experimental data of fresh and irradiated MOX thermal conductivity, including details about the fuel material and the experimental technique employed.

Fresh MOX fuel Reference	Measured fuel	Experimental technique
Bonnerot, 1988 (reported by Carbajo et al., 2001) [19]	Fresh MOX, 95% TD, [*Pu*] = 20 wt.%, O/M = 1.98, measured at *T* between 1500 and 2260 K (high temperature data).	Laser-flash method for thermal diffusivity and drop calorimetry technique for specific heat capacity; conversion to thermal conductivity. O/M determined by means of thermogravimetric and XRD analyses.
Ronchi, 1998 (reported by Carbajo et al., 2001) [19]	Fresh MOX, 95% TD, [*Pu*] = 5 wt.%, O/M = 2.00, measured at *T* between 2050 and 2700 K (high temperature data).	Laser-flash method for thermal diffusivity and drop calorimetry technique for specific heat capacity; conversion to thermal conductivity.
Staicu et al., 2013 [22]	Fresh SBR, sol-gel and MIMAS heterogeneous LWR MOX, 94.5–96% TD, [*Pu*] = 4.8 to 11.1 wt.%, O/M ~ 2.000, measured at *T* from 500 to 1550 K.	Shielded laser-flash device for thermal diffusivity, specific heat capacity assumed equal to fresh fuel values from [18, 44]; conversion to thermal conductivity. Heat treatment was used to obtain stoichiometric samples (uncertainty of 0.003).
TRABANT (ESNII+ D7.34, 2017) [24]	Fresh TRABANT MOX fuel: density from ~93 to 95% TD, [*Pu*] 40 and 45 mol.%, O/M from 1.96 to 2.00, measured at *T* between 500 and 1600 K.	Immersion technique for the density, Differential Scanning Calorimetry for the specific heat capacity, laser-flash method for the thermal diffusivity; conversion to thermal conductivity. O/M determined by thermal treatment: deduced from the pellet weight variation and checked with XRD.
PHENIX (ESNII+ D7.41, 2017) [23]	Fresh PHENIX MOX fuel: 95% TD, [*Pu*] = 24 mol.%, O/M = 2.00, measured at *T* between 500 and 1600 K.	Differential Scanning Calorimetry for the specific heat capacity, laser-flash method for the thermal diffusivity; conversion to thermal conductivity. O/M ratio measured by means of optimized thermogravimetric analysis, with uncertainty of 0.002 (at 95% confidence level).
Irradiated MOX fuel **Reference**	**Measured fuel**	**Experimental technique**
Yamamoto et al., 1993 [25]	Irradiated $(U,Pu)O_{1.97}$ (8, 19, and 35 GWd/tHM) at LHR from 12 to 38 kW/m, with fresh fuel density 93–94% TD, [*Pu*] ~18 wt.%.	Laser-flash method for thermal diffusivity, thermal conductivity obtained from thermal diffusivity, specific heat capacity and density.
NESTOR-3 (ESNII+ D7.42, 2017) [26]	Irradiated NESTOR-3 MOX fuel (84 and 130 GWd/tHM), 96% TD, [*Pu*] = 24 mol.%, O/M = 2.00, measured at *T* between 500 and 1600 K.	Laser-flash method for the simultaneous measurement of thermal diffusivity and specific heat capacity (with calorimeter in sample position); conversion to thermal conductivity.

An extensive review of experimental and modelling works dedicated to MOX melting temperature has been recently performed by Calabrese et al. [41], highlighting the importance of the oxygen-to-metal ratio for the melting behaviour of MOX fuel, especially in the high Pu concentration domain, and the prominent role played by the plutonium content in MOX fuel for fast breeder reactor applications. The effect of the O/M ratio (in the hypo-stoichiometric range), resulting from the literature review, is currently deemed negligible for burn-up values beyond 50 GWd/tHM, where the fuel stoichiometry is typically reached. For what concerns the burn-up effect on the MOX melting temperature, it is believed to saturate at high burn-up, justified by the observed decrease of soluble fission products in the fuel matrix [34]. It is indeed considered that the MOX solidus temperature decreases by 5, 4, and 3 K per 10 GWd/tHM at 50, 100 and 150 GWd/tHM, respectively, as suggested by [34], and in agreement with [25, 31]. Based on these considerations, a limited number of correlations have been developed to describe the evolution of the melting temperature of MOX fuels [6,28,31,32,42,43]. The most comprehensive correlation was proposed by Konno et al., considering the dependence on fuel plutonium and americium contents, burn-up and oxygen-to-metal ratio [32].

Considering the state of the art just recalled, the present work aims at overcoming the current limitations of thermal properties modelling of U-Pu MOX fuel in fuel performance codes. More precisely, the aim is to develop original and more comprehensive models of thermal conductivity and melting temperature of MOX fuels, applicable to fast reactor irradiation conditions, inclusive of all the fundamental dependencies (i.e., fuel temperature, burn-up, plutonium content, stoichiometry, porosity), and valid up to high temperatures, plutonium contents and burn-up, as required for several Generation IV reactor concepts. The new correlations have been first statistically assessed based on the regressor p-values to include all the effects represented by the fitting dataset, and then implemented in the TRANSURANUS fuel performance code for their integral validation against data from the HEDL P-19 fast reactor irradiation experiment. This work represents an advancement with respect to the state of the art in fuel performance codes from the property modelling point of view, towards the extension of FPCs to fast reactor conditions, validation against irradiated MOX fuel data, and application to safety analyses on Generation IV reactor concepts.

The paper is organized as follows. The correlations for fast reactor MOX thermal conductivity and melting temperature are derived, statistically assessed, validated against separate-effect MOX experimental data and compared with state-of-the-art models in Section 2 and Section 3. The integral validation against a fast reactor irradiation experiment is performed in Section 4, showing the accuracy of the code predictions with respect to measured quantities of engineering interest. Conclusions are drawn in Section 5.

2. Correlation for thermal conductivity of fast reactor MOX fuel

The first step towards the proposal of a novel thermal conductivity correlation for fast reactor MOX is the selection of the best set of experimental data, i.e., composed of measurements recently obtained from up-to-date techniques and covering wide ranges of the considered dependencies, as explained in what follows. For fresh MOX fuel, the selected thermal conductivity data are those from [22] and from PHENIX and TRABANT MOX samples (obtained in the frame of the ESNII+ Project [23,24]). These most recent datasets correspond to low temperature (up to 1650 K), deviation from stoichiometry up to 0.04 (in the hypo-stoichiometric range [24]) and Pu content ranging from 5 wt.% [22] to 45 wt.% [24], covering both the low and high-Pu regions. Given the lack of recent high-temperature data, older data from Ronchi et al. (1998) and Bonnerot et al. (1988) (reported by [19]), still considered as a reference in the field, are included in the fitting dataset. As for irradiated fast reactor MOX fuel, the recent ESNII+ Project measurements on NESTOR-3 MOX fuel [26], corresponding to high burn-up

(i.e., 84 and 130 GWd/tHM), have been selected, together with data by Yamamoto et al. [25]. The latter have been employed to derive a correlation holding also at low and moderate burn-up (samples at 8, 19 and 35 GWd/tHM). It is worth specifying that these are the only data currently accessible by the authors on thermal conductivity of irradiated fast reactor MOX fuel. Details about the MOX thermal conductivity data selected are given in Table 1.

First, a novel correlation for fresh MOX thermal conductivity (k_0) is fitted. For this purpose, a physically grounded model $k_0(T, x, [Pu], p)$ is chosen (Eq. 1). The model encompasses the three fundamental mechanisms of heat transport in a solid. The first corresponds to heat transfer via lattice vibration (phononic) and is dominant at low temperatures. The second and third term correspond to radiative and electronic heat transfer, and dominate at high temperatures. This basic model is then corrected with the inclusion of plutonium and stoichiometry-dependent terms in the lattice contribution, and of a porosity corrective factor as well. Specifically, the stoichiometry and plutonium content effects are conventionally introduced in k_0 as modifications to the A and B coefficients of the lattice vibration term (see e.g., [3,4]). Hence, the functional form of the thermal conductivity correlation for fresh MOX is:

$$k_0(T, x, [Pu], p) = \left(\frac{1}{A + BT} + CT^3 + \frac{D}{T^2}e^{-\frac{E}{T}}\right)(1-p)^{2.5} \quad (1)$$

with $A = A_0 + A_x \cdot x + A_{Pu} \cdot [Pu]$ and $B = B_0 + B_x x + B_{Pu}[Pu]$, where x is the deviation from stoichiometry ($x = 2 - O/M$, considering hypo-stoichiometric fuel), $[Pu]$ is the MOX plutonium content, while $(1-p)^{2.5}$ is the modified Loeb porosity corrective factor, adopted e.g., in the Van Uffelen-Schubert correlation, the reference model in the TRANSURANUS fuel performance code [6]. A_0, A_x, A_{Pu}, B_0, B_x, B_{Pu}, C, D, E are the coefficients to be fitted on the selected set of fresh MOX experimental data.

The linear dependency on the deviation from stoichiometry differs from the square root term proposed by a few existing correlations for MOX fuel [9,17], for UO_2 [45,46] and emerging from Molecular Dynamics calculations (e.g., [47]), but is supported by the majority of state-of-the-art models available in literature and in fuel performance codes [10,15,16,18,19]. As for the inclusion of the plutonium effect in this work, it is in contrast with previous works that excluded it, in the ranges 3–15 [18] and 15–30 [9] wt.% PuO_2. Indeed, its inclusion finds confirmation in experimental and modelling works on MOX [15,22], and also in theoretical works about thermal diffusivity and conductivity of various types of materials and nuclear fuels [48–50].

In addition to the straightforward fitting, the statistical significance and weight of each term of the correlation have been analysed and evaluated. The multi-dimensional fit has been performed using MATLAB tools [51] and the R code [52], to obtain (besides the regressor values) the associated p-values, along with the confidence intervals and the fit residuals. The significance of each term of the starting correlation has been evaluated taking the p-value associated to each regressor as figure of merit (compared to a threshold p-value of 5%, corresponding to a 95% confidence on the significance of a regressor). In this way, in the framework of a statistical hypothesis test, a regressor is kept in the final form of the correlation if the associated p-value is below 5%, otherwise it is rejected as statistically insignificant (i.e., not well represented by the fitting dataset). It is worth clarifying that the p-values obtained from the hypothesis test, like all the results of the fitting procedure, inherently depend on the chosen fitting dataset. The regressor initial values, needed by the non-linear fitting procedure, are fixed to the values employed by existing correlations for the same kind of terms [9,53,54]. The stability and independence of the resulting fit coefficients (not reported here for sake of brevity) have been tested, proving that they hold true performing further iterations and that the non-linear fitting procedure is slightly affected by their initial values.

Table 2
Results of the fit of the statistically assessed $k_0(T, x, [Pu], p)$ correlation (Eq. 2) on the whole set of fresh MOX thermal conductivity data (Table 1).

Regressor	Units	Estimate
$\mathbf{A_0}$	m•K/W	0.01926
$\mathbf{A_x}$	m•K/W	$1.06\ 10^{-6}$
$\mathbf{A_{Pu}}$	m•K/W	$2.63\ 10^{-8}$
$\mathbf{B_0}$	m/W	$2.39\ 10^{-4}$
$\mathbf{B_{Pu}}$	m/W	$1.37\ 10^{-13}$
D	W•K/m	$5.27\ 10^{+9}$
E	K	17109.5

The statistical significance of the regressors has been tested against the entire set of selected experimental data on fresh MOX (Table 1), as well as against sub-sets of the selected data, featured by at least one constant dependence amongst the parameters of interest (T, x, $[Pu]$). The aim of these partial fits is to achieve higher confidence on the significance of each correlation regressor, focusing only on the p-values. The fit of the starting k_0 over all the selected fresh MOX data shows p-values lower than 5% for the fit coefficients A_0, B_0, B_{Pu}, D, E ($< 10^{-8}$, $< 10^{-16}$, 1.5%, 4%, $< 10^{-14}$, respectively), while higher than 5% for A_x, A_{Pu}, B_x, C (39%, 10%, 46%, 25%, respectively, values depending on the experimental ranges covered by the data composing the fitting dataset). Amongst these, the regressors A_x and A_{Pu} are kept in the final formulation, since A_x has a p-value on the sub-set of (T, x)-dependent data (14%) much lower than B_x (75%), while A_{Pu} is well represented by the sub-set of (T, $[Pu]$)-dependent data (p-value lower than 5%). Additionally, the results of the partial fits confirmed the exclusion of the regressors B_x and C[2], since they are featured by p-values much higher than 5%, both on the entire set and on the sub-sets (i.e., on the sub-sets of data corresponding to low temperature and constant p and $[Pu]$, and to high temperature, respectively).

The assessed form of the novel correlation for fresh MOX thermal conductivity reads:

$$k_0(T, x, [Pu], p) = \left(\frac{1}{A_0 + A_x \cdot x + A_{Pu} \cdot [Pu] \ + (B_0 + B_{Pu}[Pu])T} + \frac{D}{T^2}e^{-\frac{E}{T}}\right)(1-p)^{2.5} \quad (2)$$

The fit of the statistically assessed k_0 (Eq. 2) on the complete set of selected fresh MOX data leads to the results collected in Table 2. The final regressor values have been obtained imposing their positivity as constraint, in order to guarantee a physically grounded significance. All the included effects degrade the thermal conductivity, as expected from experimental observations (reported in Table 1 and in other literature works, e.g., [15,20,21]) and theoretical considerations about phonon interactions with lattice defects. The coefficient values reported in Table 2 hold for T ex-

[2] The radiative contribution to the thermal conductivity, CT^3, dominates at very high temperatures, a region where the available MOX thermal conductivity experimental data are scarce. Instead, the exclusion of the regressor B_x is physically justified by the fact that B describes the phonon-phonon collisions, while A depends on impurities or alloying additions, so it is apt to include the fuel stoichiometry effect.

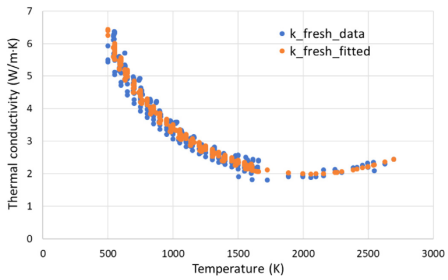

Fig. 1. Experimental data on fresh MOX thermal conductivity (considered as fit dataset, Table 1, blue dots), as a function of temperature, compared to the corresponding predictions provided by the correlation developed in this work (orange dots, Eq. 2 and Table 2). (For interpretation of the references to colour in this figure legend, the reader is referred to the web version of this article.)

pressed in K, [*Pu*] in atomic fraction, *p* in TD fraction. The thermal conductivity k_0 is calculated in W/(m•K).

The obtained effect of plutonium content and deviation from stoichiometry (in the hypo-stoichiometric range) on the MOX thermal conductivity is minor if compared to the temperature effect, as results from the coefficient values reported in Table 2. Indeed, the values of A_x, A_{Pu} and B_{Pu} are orders of magnitude lower than A_0 and B_0, which are the basic coefficients composing a lattice vibration contribution to thermal conductivity only dependent on temperature. A slight effect of the plutonium content, in the range between 0 and 45 wt.%, is supported by literature works concerning both LWR [18] and FBR MOX [9], and by the recent measurements on TRABANT fresh MOX fuel performed in the framework of the ESNII+ H2020 Project [24]. Instead, the effect of deviation from stoichiometry reveals negligible due to the lack of data points, amongst the available ones, associated to a significant hypo-stoichiometry. Indeed, most of the fresh MOX data correspond to material stoichiometry, also due to measurement conditions leading to O/M = 2.00 [22,23]. The availability of additional experimental data would allow to further assess the hypo-stoichiometry impact on the MOX thermal conductivity.

The comparison between the thermal conductivity data on which the $k_0(T, x, [Pu], p)$ correlation (Eq. 2) has been built and the fit estimations, as a function of temperature, is shown in Fig. 1. It is worth noting that the agreement between data and estimations is remarkable, both at low and high temperatures. The average residual is $2 \bullet 10^{-1}$ W/(m•K), comparable with the experimental uncertainty, which for these data is between 10% and 20% of the measured value [19,22–24]. It has been verified that the fit residuals in *T*, *x*, [*Pu*] are all randomly distributed, with no clear trends. This excludes the necessity to correct the fresh MOX thermal conductivity correlation herein derived with mixed effects terms (present in some existing thermal conductivity correlations [42,55–57]) or additional higher order terms. Such improvements would only be justified in the case of a trend of the associated residuals. Data assimilation techniques such as Bayesian calibration methods (e.g., [58]) could then be considered in the future for dealing with potential model inadequacies, when more experimental data become available.

In the following step of the model development, an exponential degradation with fuel burn-up is chosen as functional form for the thermal conductivity correlation of irradiated MOX fuel (k_{irr}, Eq. 3). This is derived from the vast amount of data generated and partly provided in the HRP [59] and IFPE [60] databases for LWR fuels

Table 3
Values of the coefficients of the $k_{irr}(T, x, [Pu], p, bu)$ correlation (Eq. 3), fitted on the set of irradiated MOX thermal conductivity data [25,26].

Regressor	Units	Estimate
$\mathbf{k_{inf}}$	W/(m•K)	1.755
φ	GWd/tHM	128.75

at extended burn-up values, pointing out the thermal conductivity degradation [61]. This is attributed to the accumulation of point defects and fission products, which increase the phonon scattering (represented by the A term in the lattice thermal conductivity model), although thermal conductivity degradation was indicated to saturate beyond approximately 50 GWd/tHM in the mid-1990s [62]. The correlation hence reads

$$k_{irr}(T, x, [Pu], p, bu) = k_{inf} + \left(k_0(T, x, [Pu], p) - k_{inf}\right) \cdot e^{-\frac{bu}{\varphi}} \qquad (3)$$

where $k_0(T, x, [Pu], p)$ is the fresh MOX thermal conductivity calculated with Eq. 2 (employing the coefficient values collected in Table 2), *bu* is the fuel burn-up in GWd/tHM, k_{inf} is the asymptotic thermal conductivity at high burn-up based on the only two available sets of experimental data on irradiated fast reactor MOX thermal conductivity [25,26], φ is the correlation coefficient fitted on [25,26] (see Table 1). This formulation is still applicable to fresh MOX fuel, since at zero burn-up $k_{irr}(T, x, [Pu], p, bu) = k_0(T, x, [Pu], p)$, from Eq. 3. The asymptotic lower limit for the thermal conductivity degradation with burn-up (k_{inf}), in principle depending on plutonium content, deviation from stoichiometry and porosity of the fuel of interest, has been fixed based on the available experimental data. Its value is derived from an extrapolation of the experimental behaviour of thermal conductivity from Yamamoto and NESTOR-3 data [25,26], at the highest common temperature of measurement (i.e., 1480 K, corresponding to the lowest thermal conductivity data), to a burn-up of 200 GWd/tHM, considered as limit fuel burn-up for Generation IV reactor applications [11,63]. The correlation coefficients are collected in Table 3, including the value of φ resulting from data fitting.

The agreement between the correlation predictions (Eq. 3) and the data of irradiated MOX thermal conductivity by Yamamoto [25], shown in Fig. 2, is satisfactory. Considering also NESTOR-3 data [26] (not reported in Fig. 2 since confidential), the overall average residual is ∼ 10%, compared to an experimental uncertainty which is ∼ 8% and ∼ 30% for NESTOR-3 and Yamamoto's datasets, respectively.

From Fig. 2, it is worth noticing that the thermal conductivity values predicted by the new correlation lie inside a 20% error band with respect to Yamamoto's experimental measurements. Moreover, the agreement is even better (10% maximum deviation) in the range of thermal conductivity values between 2 and 2.5 W/(m•K) (circled in Fig. 2), corresponding to the target temperature and burn-up conditions foreseen for Generation IV fast reactors, i.e., peak fuel temperature in excess of ∼ 2300 K and discharge fuel burn-up of 150 - 200 GWd/tHM [11,63]. The ranges of applicability of the newly developed correlations for MOX fuel thermal conductivity, corresponding to the ranges covered by the considered experimental data, are:

- Temperature, T: [500, 2700] K.
- Deviation from stoichiometry, x: [0, 0.04] (hypo-stoichiometry).
- Plutonium content, [Pu]: [0, 45] at.%.
- Porosity, p: [0, 7] %.
- Burn-up, bu: [0, 130] GWd/tHM.

The main limitation of the developed correlation is therefore the range of discharge burn-up, which may exceed 130 GWd/tHM

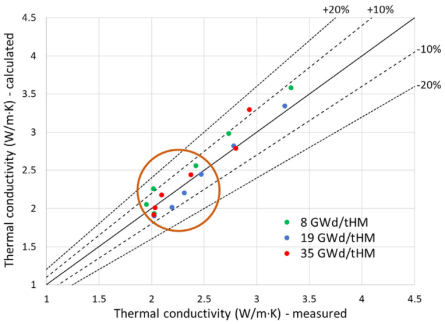

Fig. 2. Comparison between the irradiated MOX thermal conductivity data by Yamamoto [25] and the corresponding predictions given by the novel correlation for irradiated MOX (Eq. 3). The points circled in orange correspond to the range of thermal conductivity values foreseen during the operation of Generation IV reactors, for which the correlation predictions are most accurate. (For interpretation of the references to colour in this figure legend, the reader is referred to the web version of this article.)

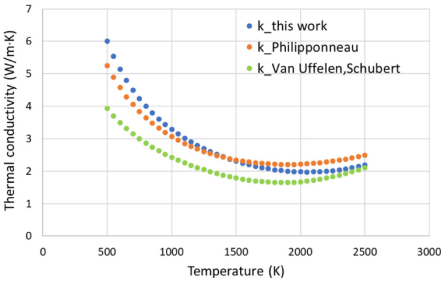

Fig. 3. Temperature behaviour of the MOX thermal conductivity correlation developed in this work (blue dots), compared to the main state-of-the-art correlations for MOX fuel (Philipponneau [9] and Van Uffelen-Schubert [6]). These values refer to stoichiometric MOX, i.e., x = 0, with 20 at.% initial Pu content and 5% porosity, at 10 GWd/tHM burn-up. (For interpretation of the references to colour in this figure legend, the reader is referred to the web version of this article.)

in Generation IV fuel types. Nevertheless, data assimilation techniques could be envisaged for a progressive upgrade of the correlation, as soon as more experimental data on representative irradiated FBR MOX fuels become available.

In Fig. 3, the behaviour of the new MOX thermal conductivity correlation as a function of fuel temperature is compared with two main correlations from literature, by Philipponneau [9] and Van Uffelen-Schubert ([6], developed for LWR MOX). Results refer to stoichiometric MOX, i.e., x = 0, with 20 at.% initial Pu content and 5% porosity, at 10 GWd/tHM burn-up. The new correlation predicts the highest thermal conductivity values at low temperature, while the three correlations all provide values between 2 and 2.5 W/(m•K) at 2500 K. Table 4 reports the root mean square errors of the three correlations considered, compared to the entire set of fitted thermal conductivity experimental data (concerning both fresh and irradiated MOX, Table 1). The error of the correlation developed in this work is less than half the error of the two state-of-the-art correlations herein considered for comparison [6,9].

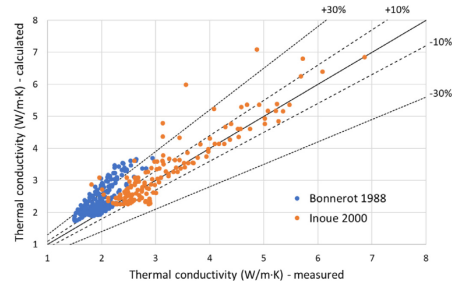

Fig. 4. Validation of the thermal conductivity correlation developed in this work against experimental data on fresh MOX, from Bonnerot [15] and reported by Inoue [17].

An independent validation of the new MOX thermal conductivity correlations is provided in Fig. 4. The sets of experimental data on fast reactor MOX considered for validation, independent from the ones composing the fitting set, are from Bonnerot [15] and Inoue [17], reporting older data on fast reactor MOX from Hetzler (1967), Van Craeynest (1968), Laskiewicz (1971), Fukushima (1983), Elbel (1985 and 1988). Bonnerot provides measurements at temperatures between 973 and 2473 K of fresh U-Pu mixed oxides, hypo-stoichiometric with O/M ratio between 1.967 and 1.99, with Pu contents from 5 wt.% to ~ 30 wt.% and porosity between ~ 3% and ~ 9%. Measurements collected by Inoue (normalized to 100% TD) concern fresh MOX fuel at temperatures between 350 and 2500 K, with Pu content from 20 to 25 wt.%, O/M ratio from 1.96 to 1.99. The cloud of points mostly lays in a 30% deviation band with respect to the experimental values, with a significant amount of predictions inside the 10% deviation region (corresponding to the best experimental uncertainty on fresh MOX thermal conductivity, from recent works [23,24]). Predicted values which over-estimate the measured ones by more than 30% correspond to the lowest temperatures of the datasets, i.e., closer to 500 K, which is the lower limit of validity of the herein proposed thermal conductivity correlation, and below the commercial range of interest for FBR MOX fuels. Instead, the agreement with data measured at high temperatures (above 1600 K), included in the operative condition range of fast and Generation IV future reactors, is remarkably good, since the maximum calculated deviation is ~ 20% of the experimental value. An independent validation against thermal conductivity data on irradiated fast reactor MOX could not be performed, since data other from those used for the fit [25,26] are not available in the open literature or not accessible to the authors. Fig. 5 shows the frequency distribution of the relative differences between the values calculated employing the MOX thermal conductivity correlation developed in this work and the experimental data, from Bonnerot [15] and Inoue [17]. For most of the correlation predictions (~ 60% and ~ 90% of the entire Bonnerot and Inoue datasets, respectively), the relative percentage error with respect to the experimental data is below 20%, hence comparable with the state-of-the-art experimental uncertainty on MOX thermal conductivity (reported between 10 and 20% of the measured value, as previously mentioned). The largest deviations are observed for the lower temperature values (between 350 and 1200 K, hence below the temperature range relevant for FBR MOX fuel during irradiation) and correspond to the points outside the 30% deviation band in Fig. 4.

Table 4
Root mean square error of the MOX thermal conductivity correlation developed in this work, compared to the main state-of-the-art correlations for MOX fuel, over the entire set of data considered in this work (both fresh and irradiated MOX, Table 1).

	Philipponneau [9]	Van Uffelen-Schubert [6]	This work
Root mean square error (rmse)	0.33	0.34	0.16

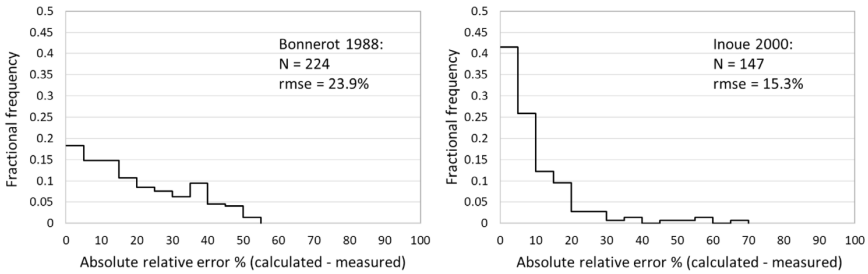

Fig. 5. Frequency distribution of the relative differences between calculated values (from the MOX thermal conductivity correlation developed in this work) and experimental data, from Bonnerot ([15], left) and Inoue ([17], right). The figure also reports the number of data points analysed and the root mean square error (rmse) of the correlation, compared to the two experimental datasets.

3. Correlation for melting temperature of fast reactor MOX fuel

The procedure employed to derive a novel, more comprehensive correlation for MOX melting temperature for fuel performance codes is similar to the one adopted for the thermal conductivity correlation. The most recent melting temperature data, obtained through reliable experimental techniques (laser heating and thermal arrest in rhenium-coated tungsten capsule), have been selected as best (most accurate) fitting dataset. In line with the considerations reported in Section 1, measurements performed on samples inside a tungsten capsule have been excluded from the fitting dataset. Moreover, data concerning MOX fuel for fast reactor applications have been considered, while allowing to cover wide ranges of plutonium contents and deviations from stoichiometry (in the hypo-stoichiometric range). Hence, as for fresh MOX, selected data (including two points from PHENIX fuel, obtained in the framework of the ESNII+ Project) are taken from [23,33,35,39,40,64]. Data from [33,39] corresponding to very high plutonium contents (> 50 wt.%) or to strong hypo-stoichiometry (around 1.90) have been excluded from the fitting dataset, since out of the range of interest of the present work (i.e., plutonium content up to 50 wt.% and deviation from stoichiometry up to 0.06). Instead, the only suitable data about irradiated fast reactor MOX are provided by Konno et al. [32][3]. The experimental points selected for the fit are collected in Table 5.

Previous experimental studies already indicated that both the plutonium content (at least up to 50 wt.%) and the deviation from stoichiometry decrease the MOX melting temperature with respect to fresh, stoichiometric UO_2 [32,34,42,53]. A recent theoretical analysis based on Molecular Dynamics calculations also confirms this effect of plutonium content in mixed oxides [65]. Therefore, a correlation with the following starting functional form for the melting temperature of fresh MOX fuel ($T_{m,0}$) has first been fitted to the selected data:

$$T_{m,0}([Pu],[Am],x) = T_{m,UO_2} - \gamma_{Pu}\,[Pu] - \gamma_{Am}\,[Am] - \gamma_x\,x \qquad (4)$$

where T_{m,UO_2} is the fresh UO_2 melting temperature (i.e., 3147 K, according to recent experimental measurements by Manara et al. [66], recommended by the ESNII+ Catalogue on MOX properties [43]), $[Pu]$ and $[Am]$ are the plutonium and americium contents (in at./), respectively, x is the deviation from fuel stoichiometry. γ_{Pu}, γ_{Am}, γ_x are the regressors associated to each effect, to be fitted on the selected fresh MOX melting temperature data. In view of the limited set of experimental data, a linear dependency on each parameter, known to affect (decrease) the melting temperature, is assumed, and each effect is considered as independent (i.e., additive to each other). An americium effect is initially considered since some of the considered works ([33], [40]) include data on Am-bearing fresh MOX fuel, which is of interest for Generation IV type of fuels. Nonetheless, the Am effect proves to be badly represented by the chosen fitting dataset (p-value greater than 5%), since too few data from too low content Am-MOX samples are available[4]. Instead, the statistical analysis (performed again through the R code [52]) indicates that the plutonium and stoichiometry effects must be included in the fresh MOX melting temperature correlation, since the p-values associated to their regressors are very low ($\sim 10^{-13}$ and 1.3%, respectively).

As a result of the statistical analysis, the proposed form of the fresh MOX melting temperature correlation reads:

$$T_{m,0}([Pu],x) = T_{m,UO_2} - \gamma_{Pu}\,[Pu] - \gamma_x\,x \qquad (5)$$

The fit of Eq. 5 over the complete fitting dataset on fresh MOX (Table 5) leads to the coefficient values reported in Table 6, holding for T_{m,UO_2} expressed in K and $[Pu]$ expressed in atomic fraction. The analysis of the residual trends does not suggest the introduction of higher order or mixed terms (instead present in Konno et al. correlation, involving, e.g., a squared dependence on the plutonium content [32]), since the fit residuals are always randomly

[3] This statement is supported by the fact that it is the only work in the open literature reporting the actual values of fuel stoichiometry and plutonium content at the sample burn-up. For this reason, melting temperature data for irradiated MOX reported by [35] have been excluded by the fitting dataset.

[4] An americium effect is represented in the Konno et al. correlation [32], based on the ideal solution model and obtained performing experimental regression analysis under the hypothesis of additive effects.

Table 5
List of selected experimental data of fresh and irradiated MOX melting temperature, including details about the fuel materials and the experimental technique employed.

Fresh MOX fuel Reference	Measured fuel	Experimental technique
Kato et al., 2008 [33]	Fresh MOX, O/M = 2.000, Pu content from 29.7 to 46.3 mol.%, Am content from 0.3 to 3.3 mol.%.	Sample heating in a rhenium capsule, analysis of pyrometer thermograms. Stoichiometric samples obtained adjusting to 2.00 by annealing at 1023 K for 5 h at the oxygen potential of ~ -400 kJ/mol.
Hirosawa et al., 2011 [35]	Fresh FR MOX with O/M = 1.99 and Pu content of 31.8 mol.%.	Sample heating in an inner rhenium capsule and outer tungsten capsule, Thermal Arrest technique. O/M measured with the oxidation–reduction gravimetric method.
Bohler et al., 2014 [39]	Fresh MOX, O/M = 2.00, Pu content from 3.7 to 50 mol.%.	Laser Heating and analysis of pyrometer thermograms. Fuel stoichiometry characterized by means of XRD, XANES and Raman analyses.
Prieur et al., 2015 [40]	Fresh MOX, O/M = 1.98, Pu content = 22 mol.%, Am content = 3.5 mol.%.	Laser Heating and analysis of pyrometer thermograms. O/M ratio determined from XANES analyses, with uncertainty of 0.01.
Strach et al., 2016 [64]	Fresh MOX, O/M = 2.00, Pu content from 14 to 54 wt.%.	Thermal Arrest technique on samples obtained from UO_2 and PuO_2 powders. Measurements in Ar atmosphere. Stoichiometry was achieved by atmosphere control during sintering and verified by powder XRD measurements.
PHENIX (ESNII+ D7.41, 2017) [23]	Fresh PHENIX MOX, 95% TD, Pu content = 24 mol.%, O/M = 2.00 (stoichiometric) and 1.978 (hypo).	Laser Heating and fast multi-channel pyrometer. O/M ratio measured by means of optimized thermogravimetric analysis, with uncertainty of 0.002 (at 95% confidence level).
Irradiated MOX fuel **Reference**	**Measured fuel**	**Experimental technique**
Konno et al. 2002 [32] **(reports also data by Tachibana et al. 1985 and Komatsu et al. 1988)**	Irradiated MOX with burn-up between 8.2 and 110.9 GWd/tHM, O/M = 1.98, Pu content ~ 17.5 mol.%, Am content between 0.13 and 0.16 mol.%.	Thermal Arrest technique on sample in a tungsten capsule. Actual values of O/M ratio of irradiated samples calculated from the given as-fabricated values, by means of a linear increasing O/M model dependent on the enrichment in ^{235}U and on burn-up.

Table 6
Results of the fit of the statistically assessed $\mathbf{T_{m,0}([Pu], x)}$ correlation (Eq. 5) on the whole set of the selected fresh MOX melting temperature data.

Regressor	Units	Estimate
γ_{Pu}	K / at./	364.85
γ_x	K	1014.15

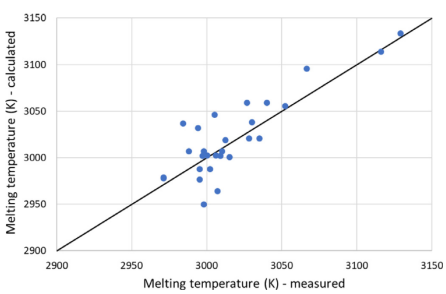

Fig. 6. Comparison between the fresh MOX melting temperature data and the corresponding predictions given by the correlation fitted on these data (Eq. 5). (For interpretation of the references to colour in this figure legend, the reader is referred to the web version of this article.)

distributed if plotted against *[Pu], [Am]* or *x*. The comparison between the experimental data and the corresponding values predicted by the new fresh MOX melting temperature correlation is shown in Fig. 6.

Fig. 6 shows that the agreement between experimental and fitted melting temperature values is acceptable, despite some relevant deviations up to 50 K. Nevertheless, the maximum residual is absolutely comparable with the high experimental uncertainty on fresh MOX melting temperature, which is between 30 and 70 K [23,33,35,39].

In a second step, the correlation for irradiated MOX melting temperature is derived by fitting a burn-up dependant function, including $T_{m,0}([Pu], x)$ (Eq. 5, with regressor values in Table 6), to the selected data for irradiated fuel [32]. To account for the burn-up effect, which also degrades the MOX melting point with respect to the fresh material [32,34,35], an exponential functional form is again adopted. This has been chosen because the effect of burn-up reflects the continuous build-up of defects and fission products, which evolves towards saturation [34], and recent Molecular Dynamics calculations of the melting temperature in mixed oxides [65] suggest a decrease of the melting temperature when a few atom percent of foreign atoms are introduced in the lattice. This has been ascribed to a decreasing Frenkel formation energy in MOX, in turn caused by a lattice mismatch due to the foreign atoms up to a few percent. The burn-up range considered in this work is of the order of few atom percent (up to ~ 110 GWd/tHM), hence the functional form chosen for the irradiated MOX melting temperature correlation is written as:

$$T_{m,irr}(bu, [Pu], x) = T_{m,inf} + \left(T_{m,0} - T_{m,inf}\right) \cdot e^{-\frac{bu}{\delta}} \quad (6)$$

where *bu* is the fuel burn-up in GWd/tHM, $T_{m,0}$ is the melting temperature of the fresh fuel according to Eq. 5, while $T_{m,inf}$ and δ are the correlation regressors to be fitted. This formulation is consistent with $T_{m,irr} = T_{m,0}$ when the fuel burn-up is equal to zero. Fitting this functional form to the irradiated MOX data [32] leads to the regressor values reported in Table 7. The comparison between the values predicted by the new correlation (Eq. 6) and the corresponding experimental values is shown in Fig. 7. The average deviation from the experimental data is around 15 K, comparable with the experimental uncertainty reported for irradiated MOX melting temperature (between 10 and 30 K) [32]. The agreement between calculated and measured values is even better considering the experimental uncertainties, as most of the error bars reported in Fig. 7 include the perfect agreement, represented by the plot diagonal. The ranges of applicability of the newly developed correlations for MOX fuel melting temperature, corresponding to the ranges covered by the considered experimental data, are:

Table 7
Results of the fit of the $\mathbf{T_{m,\,irr}}$(**bu**, [**Pu**], **x**) correlation (Eq. 6) over the selected irradiated MOX melting temperature data.

Regressor	Units	Estimate
$\mathbf{T_{m,inf}}$	K	2964.92
δ	GWd/tHM	40.43

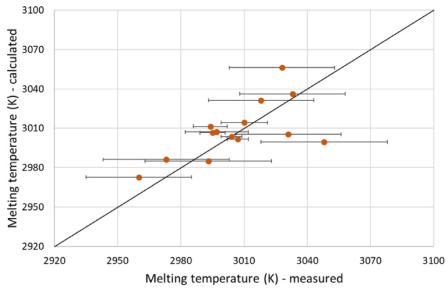

Fig. 7. Comparison between the irradiated MOX melting temperature data and the corresponding predictions given by the correlation fitted on these data (Eq. 6). The experimental uncertainties, as provided by the original references [30–32], are included as horizontal error bars. (For interpretation of the references to colour in this figure legend, the reader is referred to the web version of this article.)

- Deviation from stoichiometry, x: [0, 0.06] (hypo-stoichiometry).
- Plutonium content, [Pu]: [0, 50] at.%.
- Burn-up, bu: [0, 110] GWd/tHM.

In Fig. 8, the behaviour of the MOX melting temperature correlation derived in this work, as a function of (a) plutonium content (considering stoichiometric fuel at 10 GWd/tHM) and (b) fuel burn-up (considering stoichiometric fuel with 30 at.% initial Pu content), is compared with two main state-of-the-art correlations, Konno et al. [32] and MATPRO ([42], valid for UO_2 and LWR MOX). The behaviour of the two state-of-the-art correlations considered for comparison is sensibly different and predicted values differ by more than one hundred degrees. The new correlation for $T_{m,\,irr}$ provides values between the two state-of-the-art correlations, especially in terms of plutonium degradation effect. The effect of plutonium in the MATPRO correlation is negligible, while Konno et al. correlation is featured by a stronger degradation (decrease) of the predicted melting temperature with increasing plutonium content (at 10 GWd/tHM burn-up, as showcased in Fig. 8a). This could be due to the fact that the plutonium content effect in the Konno et al. correlation [32] is based on quite old and low (down to 2850 K at 50 at.% Pu) experimental data on MOX fuels, provided by Lyon and Baily [27] and by Aitken and Evans [28]. The burn-up effect is derived by Konno by fitting Japanese experimental data from JOYO reactor campaigns, reported in his same work [32]. Instead, the novel correlation herein proposed is based on a wider dataset, composed of recent and up-to-date literature works from various authors (including Konno's data for the burn-up effect), showing experimental data of MOX melting temperature which are higher in value (never lower than 2950 K, as shown in Figs. 6 and 7). The correlation developed in this work is featured by its characteristic decreasing exponential trend in burn-up (Eq. 6), which leads to higher predicted values at high burn-up. This could be justified by the fact that, at such burn-up values, either the high burn-up structure formation in the low temperature fuel region is accompanied by a reduction of the fission products in the lattice (observed by means of EPMA [67–69]), or a large fractional release of fission products occurs in FBR MOX fuels in the high temperature region. Table 8 reports the root mean square errors of the

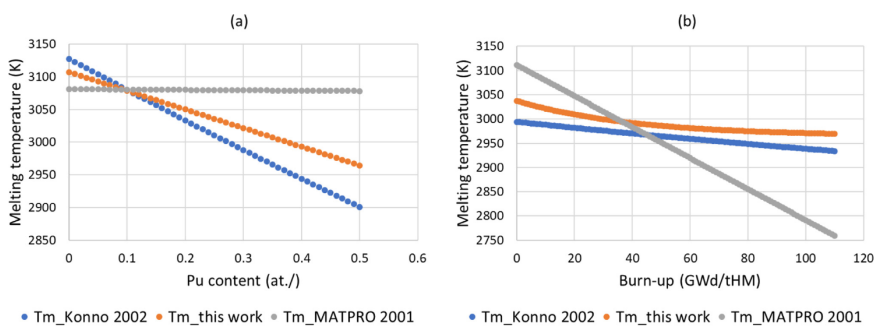

Fig. 8. Behaviour of the MOX melting temperature correlation herein presented (blue dots), as a function of (a) plutonium content and (b) burn-up, compared to two main state-of-the-art correlations for MOX fuel (Konno et al. [32] and MATPRO [42]). The calculated values, in both graphs, refer to stoichiometric MOX, i.e., x = 0, while in (a) bu = 10 GWd/tHM and in (b) [Pu] = 30 at.%. (For interpretation of the references to colour in this figure legend, the reader is referred to the web version of this article.)

Table 8
Root mean square error of the MOX melting temperature correlation developed in this work, compared to the main state-of-the-art correlations for MOX fuel, over the entire set of herein considered data on fresh and irradiated MOX (Table 5).

	Konno et al. [32]	MATPRO [42]	This work
Root mean square error (rmse)	0.014	0.029	0.0065

Table 9
Details about the as-fabricated geometry, materials and boundary conditions of the fuel rods irradiated in the HEDL P-19 experiment (TD = Theoretical Density, OD = Outer Diameter, LHR = Linear Heat Rate).

Rod ID	3	6	7	8	13	20	24	25	26	27	28	30	33	35
Gap size (μm)	127	49.5	79	122	99	123	127	101.5	76	51	43	89	62.5	91.5
Density (%TD)	92.4	90.75	92.4	90.75	90.75	90.75	92.4	92.4	92.4	92.4	92.4	92.4	90.75	90.75
Clad OD (mm)	6.35	5.84	6.35	5.84	5.84	5.84	6.35	6.35	6.35	6.35	6.35	6.35	5.84	5.84
Fuel	25% PuO_2 – 75% UO_2													
Cladding	AISI 316 stainless steel (20% cold-worked)													
Filling gas	98% He, 2% Ar at 1 bar													
O/M	1.96													
Active fuel length	343 mm													
Na inlet temperature	640 K													
Max LHR (kW/m)	64	56.1	66.6	53.8	54.5	54.1	64.6	66	66.9	66.9	67.9	65.6	55.1	54.1
Melting	X		X	X	X	X	X	X	X	X	X	X		X

three correlations considered, when compared to the entire set of herein considered experimental data, both on fresh and irradiated MOX fuel (Table 5). The error of the correlation developed in this work is much lower than the error of the two main state-of-the-art correlations [32,42] over the considered data.

4. Application to the HEDL P-19 irradiation experiment and integral validation

The correlations for MOX thermal conductivity and melting temperature developed in this work have been implemented in the TRANSURANUS fuel performance code, for their assessment against available integral data (i.e., at the fuel pin level). The effect of the new correlations on fuel pin performance simulations has been tested against experimental data from the HEDL P-19 irradiation experiment, and the TRANSURANUS results are discussed in what follows.

HEDL P-19 is a fast reactor irradiation experiment performed in 1971 in the EBR-II reactor (sodium-cooled, open pool type) [70]. It is a power-to-melt test with the objective to investigate the melting propensity of 25% PuO_2, fresh MOX fuel, representative of FBR pin design. The experiment aimed to simulate fast start-up situations, typical of FBRs. The irradiation history consisted in a starting slow power ramp (10 hours long, up to 85% of the reactor total power, i.e., 62.5 MW), after which this steady power level is kept for 2 hours. After the conditioning phase, the reactor is rapidly ramped up to full power, which is kept for ~ 10 minutes, followed by reactor scram. The maximum burn-up reached by the fuel in this experiment is ~ 1 GWd/tHM. Experimental data on 14 pins are available in the HEDL P-19 database, regarding the power-to-melt (i.e., the linear power leading to incipient fuel melting, measured at the top and bottom of fuel column), which is the main outcome of interest from the experiment; the radial and axial extents of fuel melting, and some PIE data about the central void size, the radial extent of the columnar grain region and the fuel-to-cladding gap size [70–72]. Table 9 summarizes the main relevant as-fabricated details and boundary conditions of the HEDL P-19 fuel rods.

The simulation of the HEDL P-19 irradiation experiment has been performed with the v1m1j18 version of the TRANSURANUS fuel performance code. The results obtained employing the new thermal conductivity and melting temperature correlations for fast reactor MOX are validated against experimental data and compared with the results from state-of-the-art correlations implemented in TRANSURANUS (i.e., the Van Uffelen-Schubert correlation for MOX thermal conductivity [6]; as for the melting temperature, a fixed, experimental value of 3035 K is considered, which was measured during the HEDL P-19 campaign and provided in the experimental reports [70,71,73]). The aim of this analysis is to quantify the improvement in the code predictions on integral quantities brought about by the new correlations, besides validating them for use in fuel performance codes and for application to MOX fuel in fast reactor conditions.

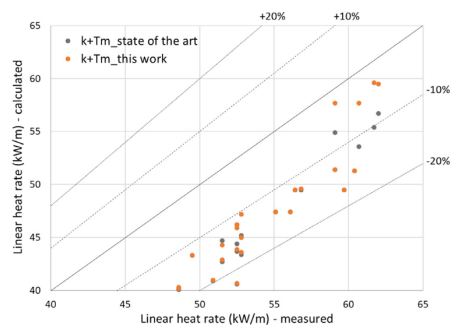

Fig. 9. Integral validation (orange points) of the new thermal conductivity and melting temperature correlations for fast reactor MOX against power-to-melt data from the HEDL P-19 irradiation experiment [70]. The results obtained employing state-of-the-art TRANSURANUS correlations are also reported (grey points), for sake of comparison. Where grey points are not visible, they are exactly covered by orange points. (For interpretation of the references to colour in this figure legend, the reader is referred to the web version of this article.)

The integral validation against the HEDL P-19 power-to-melt data is reported in Fig. 9, showing generally consistent diagonal trends (higher the experimental data, higher the corresponding calculated value). Predictions are mostly similar, but for some HEDL pins more accurate (closer to the plot diagonal, i.e., to the perfect agreement with the data) from the new thermal conductivity and melting temperature correlations. Despite the predicted values are contained within the 20% error band from the experimental values, the power-to-melt data are systematically underestimated by TRANSURANUS, indicating the conservative behaviour of the code. Anyway, the experimental uncertainty on the power-to-melt measurements, which is reported equal to 6% [70], must be considered in order to evaluate the accuracy of the TRANSURANUS calculations, along with the uncertainties pertaining to the gap conductance and relocation modelling at beginning of life, as pointed out recently in a code benchmark of the OECD/NEA and in the ESFR-SMART Euratom project [74,75].

Fig. 10 shows the integral validation against HEDL P-19 post-irradiation examination data, concerning the maximum radial extent of fuel melting (measured at the peak power node, left plot) and the fuel-cladding gap size (right plot). As for the fuel radial melting extent, a general over-estimation of the experimental data can be noticed, which is consistent with the under-estimation of

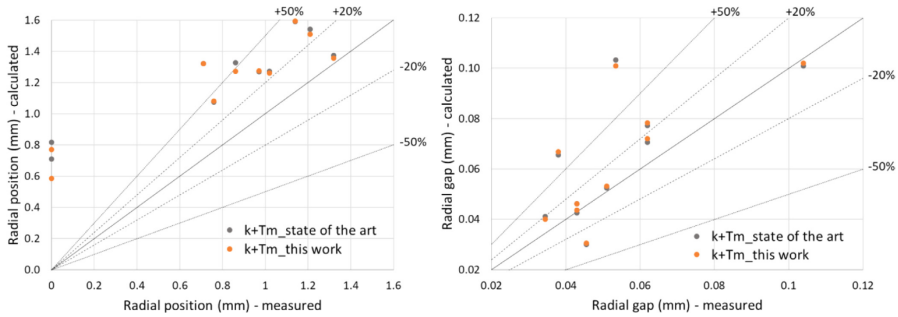

Fig. 10. Integral validation of the new thermal conductivity and melting temperature correlations for fast reactor MOX against radial melting extent data (left plot) and fuel-cladding gap size data (right plot), at end-of-life, from the HEDL P-19 irradiation experiment [70]. The results obtained employing state-of-the-art TRANSURANUS correlations are also reported, for sake of comparison. Where grey points are not visible, they are exactly covered by orange points. (For interpretation of the references to colour in this figure legend, the reader is referred to the web version of this article.)

the power-to-melt. This is also consistent with the over-estimation (for all the experimentally melted pins) of the axial melting extent, employing both sets of correlations. Moreover, the code predicts melting (both radial, as shown in Fig. 10 - left, and axial) also for two rods (number 6 and 33, from Table 9) which experimentally are un-melted after the irradiation. The new correlations again provide slightly more accurate predictions with respect to the state-of-the-art. Instead, regarding the final fuel-cladding gap size, no significant improvement can be noticed from the new correlations, since calculated values are very similar. Nevertheless, the gap size is determined by many different phenomena occurring in a fuel rod (e.g., fuel relocation, fuel and cladding swelling and creep), overruling the effect of thermal conductivity and melting temperature models. The less accurate predictions, outside the 50% error band, correspond to those HEDL P-19 pins with the highest as-fabricated gap size, where the aforementioned model uncertainties on fuel relocation and gap conductance dominate.

5. Conclusions

In this work, novel and more comprehensive correlations for the thermal conductivity and melting temperature of fast reactor MOX have been developed, fitting recent and reliable experimental data to obtain models that contain all the fundamental effects (i.e., fuel temperature, burn-up, plutonium content, deviation from stoichiometry, porosity). The functional form of these new correlations has been statistically assessed through a p-value analysis, which confirmed the inclusion of the aforementioned dependencies in both models. The validity ranges have been extended with respect to state-of-the-art correlations, now reaching higher temperatures (up to 2700 K, for the thermal conductivity correlation), higher plutonium contents (up to 50 at.%) and higher burn-up (up to 130 GWd/tHM). Moreover, the correlations herein proposed have been validated against experimental measurements, with encouraging results, affected by deviations from the measured data generally comparable with the experimental uncertainties.

Additionally, the novel MOX thermal conductivity and melting temperature correlations have been implemented in the TRANSURANUS fuel performance code, for validation against integral data from the HEDL P-19 irradiation experiment, concerning MOX fuel in fast reactor start-up conditions. The new correlations show a promising predictive capability of both integral and local experimental data from post-irradiation examinations, improving or at least matching the predictions from state-of-the art correlations. The code calculations are generally conservative with respect to the experimental measurements, since the power-to-melt is under-estimated, and the fuel axial and radial melting extents are over-estimated.

This work represents a step towards the extension, improvement and validation of fuel performance codes for application to safety analyses on fast reactor MOX fuels, of great interest in the framework of Generation IV reactor concepts development. Additional experimental measurements and uncertainty indications will help to both further improve and validate the novel models herein presented (for what concerns e.g., the effect of hypo-stoichiometry and burn-up on the thermal conductivity), along with data assimilation techniques. As a complement, values calculated from Molecular Dynamics simulations could further help in supporting and interpreting experimental data. As potential future model improvement, the development of a mechanistic approach to thermal conductivity is of great interest, to increase the physical ground of the model developed in this work. To this end, one could consider either the fission product concentration remaining in the fuel or an effective fuel burn-up, to account for the effect of annealing of the irradiation damage and fission product removal at high temperatures (typical for fast reactor MOX) in the present model. Moreover, the mechanistic approach would be applicable to different nuclear fuel materials (e.g., minor actinide-bearing fuels, relevant for fast breeder Generation IV applications) and different thermal properties (e.g., thermal diffusivity, heat capacity). Finally, uncertainty and sensitivity analyses on the thermal properties herein investigated, which currently are still at preliminary stages for fuel performance codes, are planned, given their fundamental role in the development of fast reactor Generation IV concepts employing MOX nuclear fuel.

Declaration of Competing Interest

The authors declare that they have no known competing financial interests or personal relationships that could have appeared to influence the work reported in this paper.

Acknowledgments

This work has received funding from the Euratom research and training programme 2014–2018 through the INSPYRE project under grant agreement No 754329.

References

[1] M. Bertolus, "INSPYRE - Investigations Supporting MOX Fuel Licensing in ESNII Prototype Reactors", 2017. [Online]. Available: http://www.eera-jpnm.eu/inspyre/.
[2] D.R. Olander, Fundamental Aspects of Nuclear Reactor Fuel Elements, 1976.
[3] P. Van Uffelen, R.J.M. Konings, C. Vitanza, J. Tulenko, Analysis of reactor fuel rod behavior, in: D.G. Cacuci (Ed.), Handbook of Nuclear Engineering, Springer Science + Business Media, LLC, New York, NY, USA, 2010, pp. 1519–1627.
[4] P. Van Uffelen, M. Suzuki, Oxide fuel performance modeling and simulations, in: Comprehensive Nuclear Materials, 3, Elsevier Inc., 2012, pp. 535–577.
[5] M. Lainet, B. Michel, J.C. Dumas, M. Pelletier, I. Ramière, GERMINAL, a fuel performance code of the PLEIADES platform to simulate the in-pile behaviour of mixed oxide fuel pins for sodium-cooled fast reactors, J. Nucl. Mater. 516 (2019) 30–53.
[6] European Commission, TRANSURANUS Handbook, 2017.
[7] J.D. Hales et al., *BISON Theory Manual: the Equations behind Nuclear Fuel Analysis*, Tech. Rep. INL/EXT-13-29930, Rev. 1, Idaho Falls, ID, USA, 2014.
[8] Y. Udagawa, M. Amaya, Model updates and performance evaluations on fuel performance code FEMAXI-8 for light water reactor fuel analysis, J. Nucl. Sci. Technol. 56 (6) (2019) 461–470.
[9] Y. Philipponneau, Thermal conductivity of $(U, Pu)O_{2-x}$ mixed oxide fuel, J. Nucl. Mater. 188 (1992) 194–197.
[10] K.J. Geelhood, W.G. Luscher, FRAPCON-3.5: A Computer Code for the Calculation of Steady-State, Thermal-Mechanical Behavior of Oxide Fuel Rods for High Burnup, 1, 2014 NUREG/CR-7.
[11] GIF (Generation IV International Forum), 2019 Annual Report, NEA No. 7527, OECD 2020 (https://www.gen-4.org/gif/jcms/c_119024/gif-2019-annual-report).
[12] G. Locatelli, M. Mancini, N. Todeschini, Generation IV nuclear reactors: Current status and future prospects, Energy Policy 61 (2013) 1503–1520.
[13] D.R. Olander, Nuclear fuels - Present and future, J. Nucl. Mater. 389 (1) (2009) 1–22.
[14] R.L. Gibby, The effect of plutonium content on the thermal conductivity of $(U, Pu)O_2$ solid solutions, J. Nucl. Mater. 38 (1971) 163–177.
[15] J.-M. Bonnerot, Propriétés thermiques des oxydes mixtes d'uranium et de plutonium, PhD thesis, 1988.
[16] D.G. Martin, A re-appraisal of the thermal conductivity of UO_2 and mixed (U, Pu) oxide fuels, J. Nucl. Mater. 110 (1) (1982) 73–94.
[17] M. Inoue, Thermal conductivity of uranium-plutonium oxide fuel for fast reactors, J. Nucl. Mater. 282 (2–3) (2000) 186–195.
[18] C. Duriez, J.P. Alessandri, T. Gervais, Y. Philipponneau, Thermal conductivity of hypostoichiometric low pu content $(U, Pu)O_{2-x}$ mixed oxide, J. Nucl. Mater. 277 (2–3) (2000) 143–158.
[19] J.J. Carbajo, G.L. Yoder, S.G. Popov, V.K. Ivanov, A review of the thermophysical properties of MOX and UO_2 fuels, J. Nucl. Mater. 299 (3) (2001) 181.
[20] C. Cozzo, D. Staicu, G. Pagliosa, D. Papaioannou, V.V. Rondinella, R.J.M. Konings, C.T. Walker, M.A. Barker, P. Hervé, Thermal diffusivity of homogeneous SBR MOX fuel with a burn-up of 35 MWd/kgHM, J. Nucl. Mater. 400 (3) (2010) 213–217.
[21] D. Staicu, C. Cozzo, G. Pagliosa, D. Papaioannou, S. Bremier, V.V. Rondinella, C.T. Walker, A. Sasahara, Thermal conductivity of homogeneous and heterogeneous MOX fuel with up to 44 MWd/kgHM burn-up, J. Nucl. Mater. 412 (1) (2011) 129–137.
[22] D. Staicu, M. Barker, Thermal conductivity of heterogeneous LWR MOX fuels, J. Nucl. Mater. 442 (1–3) (2013) 46–52.
[23] D. Staicu et al., Preparing ESNII for HORIZON 2020 - Deliverable D7.4.1 - Measurement of properties of fresh Phenix fuel, ESNII+ Deliverable, 2017.
[24] D. Staicu et al., Preparing ESNII for HORIZON 2020 - Deliverable D7.3.4 - Characterization and measurement of properties of fresh TRABANT fuel, ESNII+ Deliverable, 2017.
[25] K. Yamamoto, T. Hirosawa, K. Yoshikawa, K. Morozumi, S. Nomura, Melting temperature and thermal conductivity of irradiated mixed oxide fuel, J. Nucl. Mater. 204 (C) (1993) 85–92.
[26] D. Staicu, E. Dahms, T. Wiss, O. Benes, and J. Colle, Preparing ESNII for HORIZON 2020 - Deliverable D7.4.2 - Properties measurements on irradiated fuels (NESTOR 3), ESNII+ Deliverable, 2017.
[27] L. Lyon, E. Baily, The solid-liquid phase diagram for the UO_2-PuO_2, J. Nucl. Mater. 22 (10) (1967) 332–339.
[28] M.G. Adamson, E.A. Aitken, R.W. Caputi, Experimental and thermodynamic evaluation of the melting behavior of irradiated oxide fuels, J. Nucl. Mater. 130 (C) (1985) 349–365.
[29] M. Kato, K. Morimoto, H. Sugata, K. Konashi, M. Kashimura, T. Abe, Solidus and liquidus of plutonium and uranium mixed oxide, J. Alloys Compd. 452 (1) (2008) 48–53.
[30] T. Tachibana, T. Ohmori, S. Yamanouchi, T. Itaki, Determination of melting point of mixed-oxide fuel irradiated in fast breeder reactor, J. Nucl. Sci. Technol. 22 (2) (1985) 155–157.
[31] J. Komatsu, T. Tachibana, K. Konashi, The melting temperature of irradiated oxide fuel, J. Nucl. Mater. 154 (1) (1988) 38–44.
[32] K. Konno, T. Hirosawa, Melting temperature of mixed oxide fuels for fast reactors, J. Nucl. Sci. Technol. 39 (7) (2002) 771–777.
[33] M. Kato, K. Morimoto, H. Sugata, K. Konashi, M. Kashimura, T. Abe, Solidus and liquidus temperatures in the UO_2-PuO_2 system, J. Nucl. Mater. 373 (1–3) (2008) 237–245.
[34] K. Konno, T. Hirosawa, Melting temperature of irradiated fast reactor mixed oxide fuels, J. Nucl. Sci. Technol. 35 (7) (1998) 494–501.
[35] T. Hirosawa, I. Sato, Burnup dependence of melting temperature of FBR mixed oxide fuels irradiated to high burnup, J. Nucl. Mater. 418 (1–3) (2011) 207–214.
[36] F. De Bruycker, K. Boboridis, D. Manara, P. Pöml, M. Rini, R.J.M. Konings, Reassessing the melting temperature of PuO_2, Mater. Today 13 (11) (2010) 52–55.
[37] D. Manara, R. Böhler, K. Boboridis, L. Capriotti, A. Quaini, L. Luzzi, F. De Bruycker, C. Guéneau, N. Dupin, R.J.M. Konings, The Melting Behaviour of Oxide Nuclear Fuels: Effects of the Oxygen Potential Studied by Laser Heating, Procedia Chem 7 (2012) 505–512.
[38] F. De Bruycker, K. Boboridis, R.J.M. Konings, M. Rini, R. Eloirdi, C. Guéneau, N. Dupin, D. Manara, On the melting behaviour of uranium/plutonium mixed dioxides with high-Pu content: A laser heating study, J. Nucl. Mater. 419 (1–3) (2011) 186–193.
[39] R. Böhler, M.J. Welland, D. Prieur, P. Cakir, T. Vitova, T. Pruessmann, I. Pidchenko, C. Hennig, C. Guéneau, R.J.M. Konings, D. Manara, Recent advances in the study of the UO_2-PuO_2 phase diagram at high temperatures, J. Nucl. Mater. 448 (1–3) (2014) 330–339.
[40] D. Prieur, R.C. Belin, D. Manara, D. Staicu, J.-C. Richaud, J.-F. Vigier, A.C. Scheinost, J. Somers, P. Martin, Linear thermal expansion, thermal diffusivity and melting temperature of Am-MOX and Np-MOX, J. Alloys Compd. 637 (2015) 326–331.
[41] R. Calabrese, D. Manara, A. Schubert, J. Van De Laar, P. Van Uffelen, Melting temperature of MOX fuel for FBR applications: TRANSURANUS modelling and experimental findings, Nucl. Eng. Des. 283 (2015) 148–154.
[42] L.J. Siefken, E.W. Coryel, E.A. Harvego, J.K. Hohorst, SCDAP/RELAP5/MOD 3.3 Code Manual, MATPRO - A Library of Materials Properties For Light-Water-Reactor Accident Analysis, 4, 2001.
[43] P. Martin et al., Preparing ESNII for HORIZON 2020 - Deliverable D7.5.1 - Catalog on MOX properties for fast reactors, ESNII+ Deliverable, 2017.
[44] J. Fink, Thermophysical properties of uranium dioxide, J. Nucl. Mater. 279 (1) (2000) 1–18.
[45] W.E. Ellis, J.D. Porter, T.L. Shaw, The effect of oxidation, burnup and poisoning on the thermal conductivity of UO_2: a comparison of data with theory, in: Proc. of LWRFP meeting, 10-13 April 2000, Park City, Utah, USA, 2000, pp. 1–15.
[46] A.R. Massih, UO_2 fuel oxidation and fission gas release, Swedish Radiation Safety Authority report, Report number: 2018:25, 2018.
[47] A. Resnick, K. Mitchell, J. Park, E.B. Farfán, T. Yee, Thermal transport study in actinide oxides with point defects, Nucl. Eng. Technol. 51 (5) (2019) 1398–1405.
[48] C. Cozzo, D. Staicu, J. Somers, A. Fernandez, R.J.M. Konings, Thermal diffusivity and conductivity of thorium-plutonium mixed oxides, J. Nucl. Mater. 416 (1–2) (2011) 135–141.
[49] M. Saoudi, D. Staicu, J. Mouris, A. Bergeron, H. Hamilton, M. Naji, D. Freis, M. Cologna, Thermal diffusivity and conductivity of thorium- uranium mixed oxides, J. Nucl. Mater. 500 (2018) 381–388.
[50] D. Jain, C.G.S. Pillai, B.S. Rao, R.V. Kulkarni, E. Ramdasan, K.C. Sahoo, Thermal diffusivity and thermal conductivity of thoria-lanthana solid solutions up to 10 mol.% $LaO_{1.5}$, J. Nucl. Mater. 353 (1–2) (2006) 35–41.
[51] MathWorks, "MATLAB code", 2019. [Online]. Available: https://uk.mathworks.com/products/matlab.html.
[52] The R Foundation, "R version 3.5.1″, 2018. [Online]. Available: https://www.r-project.org/.
[53] K. Lassmann, A. Schubert, P. Van Uffelen, C. Gyori, J. van de Laar, TRANSURANUS Handbook, Copyright © 1975-2014, Institute for Transuranium Elements, Karlsruhe, Germany, 2014.
[54] M. Suzuki, H. Saitou, Y. Udagawa, F. Nagase, Light Water Reactor Fuel Analysis Code FEMAXI-7; Model and Structure, (July 2013).
[55] B. Lee, Y. Koo, D. Sohn, Modelling of MOX fuel's thermal conductivity considering its microstructural heterogeneity, in: IAEA Technical Committee meeting, Windermere, United Kingdom, , 2000, pp. 247–256.
[56] M. Teague, M. Tonks, S. Novascone, S. Hayes, Microstructural modeling of thermal conductivity of high burn-up mixed oxide fuel, J. Nucl. Mater. 444 (1–3) (2014) 161–169.
[57] M. Amaya, J. Nakamura, F. Nagase, T. Fuketa, Thermal conductivity evaluation of high burnup mixed-oxide (MOX) fuel pellet, J. Nucl. Mater. 414 (2) (2011) 303–308.
[58] P. Pernot, F. Cailliez, A critical review of statistical calibration/prediction models handling data inconsistency and model inadequacy, AIChE J 63 (10) (2017) 4642–4665.
[59] OECD/NEA, "NEA Halden Reactor Project", 2019. [Online]. Available: https://www.oecd-nea.org/jointproj/halden.html.
[60] OECD/NEA, "International Fuel Performance Experiments (IFPE) database", 2017. [Online]. Available: https://www.oecd-nea.org/science/wprs/fuel/ifpelst.html.
[61] E. Kolstad, C. Vitanza, Fuel rod and core materials investigations related to LWR extended burnup operation, J. Nucl. Mater. 188 (1992) 104–112.
[62] D. Baron, About the modelling of fuel thermal conductivity degradation at high-burnup accounting for recovering process with temperature, in: Proc. Seminar on Thermal Performance of High Burn-up LWR Fuel, OECD-NEA, 3-6 March 1998, Cadarache, France, 1998.
[63] Institut de Radioprotection et de Sureté Nucléaire, Review of Generation IV Nuclear Energy Systems, 2015.

[64] M. Strach, D. Manara, R.C. Belin, J. Rogez, Melting behavior of mixed U-Pu oxides under oxidizing conditions, Nucl. Instruments Methods Phys. Res. Sect. B Beam Interact. with Mater. Atoms 374 (2016) 125–128.
[65] C.O.T. Galvin, P.A. Burr, M.W.D. Cooper, P.C.M. Fossati, R.W. Grimes, Using Molecular Dynamics to Predict the Solidus and Liquidus of Mixed Oxides $(Th,U)O_2$, $(Th,Pu)O_2$ and $(Pu,U)O_2$, J. Nucl. Mater. 534 (2020) 152127.
[66] D. Manara, C. Ronchi, M. Sheindlin, M. Lewis, M. Brykin, Melting of stoichiometric and hyperstoichiometric uranium dioxide, J. Nucl. Mater. 342 (1–3) (2005) 148–163.
[67] C.T. Walker, Assessment of the radial extent and completion of recrystallisation in high burn-up UO_2 nuclear fuel by EPMA, J. Nucl. Mater. 275 (1) (1999) 56–62.
[68] J. Noirot, L. Desgranges, J. Lamontagne, Detailed characterization of high burn-up structures in oxide fuels, J. Nucl. Mater. 372 (2–3) (2008) 318–339.
[69] F. Lemoine, D. Baron, P. Blanpain, Key parameters for the High Burnup Structure formation thresholds, in: Proc. 2010 LWR Fuel Performance Meeting/Top Fuel/WRFPM, 26-29 September 2010, Orlando, Florida, USA, 2010.
[70] R.B. Baker, Integral Heat Rate-to-incipient Melting in UO_2-PUO_2 Fast Reactor Fuel, Report HEDL-TME 77-23, 1978.
[71] A. Aly, C. Demaziere, D. Rozzia, A. Del Nevo, On the Effect of MOX Fuel Conductivity in Predicting Melting in FR Fresh Fuel by Means of TRANSURANUS Code, in: 24th International Conference Nuclear Energy for New Europe (NENE2015), 2015, pp. 1–9.
[72] R. Calabrese, A. Schubert, P. Van Uffelen, TRANSURANUS Code Performance under Fuel Melting Conditions: the HEDL P-19 Experiment, in: 25th International Conference Nuclear Energy for New Europe (NENE2016), 2016, pp. 1–8.
[73] D. Rozzia, A. Del Nevo, A. Ardizzone, M. Tarantino, P. Agostini, Capabilities of TRANSURANUS Code in Simulating Inception of Melting in FBR MOX Fuel, in: 22nd International Conference Nuclear Energy for New Europe (NENE2013), 2013, pp. 1–8.
[74] J. Lavarenne, et al., A 2-D correlation to evaluate fuel-cladding gap thermal conductance in mixed oxide fuel elements for sodium-cooled fast reactors, in: Proceedings of Global/Top Fuel 2019, 22-27 September 2019, Seattle, Washington, USA, 2019.
[75] N. Chauvin, et al., Benchmark study on Fuel Performance Codes for Fast Reactor, in: Proc. Int. Conf. Global/Top Fuel 2019, 22-26 September 2019, Seattle, Washington, USA, 2019.